
Masters Theses

Student Theses and Dissertations

1952

Photoelastic investigation of notched corners in square apertures in flat plates subjected to tension

Lloyd E. Byrd Jr.

Follow this and additional works at: https://scholarsmine.mst.edu/masters_theses



Part of the [Mechanical Engineering Commons](#)

Department:

Recommended Citation

Byrd, Lloyd E. Jr., "Photoelastic investigation of notched corners in square apertures in flat plates subjected to tension" (1952). *Masters Theses*. 2045.

https://scholarsmine.mst.edu/masters_theses/2045

This thesis is brought to you by Scholars' Mine, a service of the Missouri S&T Library and Learning Resources. This work is protected by U. S. Copyright Law. Unauthorized use including reproduction for redistribution requires the permission of the copyright holder. For more information, please contact scholarsmine@mst.edu.

T 1013
c. 1

PHOTOELASTIC INVESTIGATION OF NOTCHED CORNERS
IN SQUARE APERTURES IN FLAT PLATES SUBJECTED
TO TENSION

BY
LLOYD E. BYRD, Jr.

A
THESIS
submitted to the faculty of the
SCHOOL OF MINES AND METALLURGY OF THE UNIVERSITY OF MISSOURI
in partial fulfillment of the work required for the
Degree of
MASTER OF SCIENCE, MECHANICAL ENGINEERING MAJOR
Rolla, Missouri
1952



82638

Approved by

Clarence Miles
Professor of Mechanical Engineering

CONTENTS

	Page
List of illustrations	ii
List of plates	iii
List of tables	iv
Notations	v
Introduction	1
History	3
Optics	4
Stress	12
Problem and procedure	14
Photographs and data	17
Conclusions	27
Bibliography	28
Vita	29

LIST OF ILLUSTRATIONS

Fig.		Page
1.-5.	Sketches showing the determination of polarized light components	4-9
6.	Sketch showing stresses at a point in a two-dimensional system	12
7.	Sketch of model	16
8.-17.	Photographs of models	17-21

LIST OF PLATES

Plate		Page
1.	Stress concentration factors for varying notch diameters	25
2.	Stress concentration factors for varying hole sizes	26

LIST OF TABLES

Table	Page
1. Data for the models in the first test	23
2. Data for the models in the second test	24

NOTATIONS

α	Amplitude of vibration
ω	Angular velocity
A	Light vector
V	Velocity of light
N	Index of refraction
d	Model thickness
f	Wave lengths
c	Photoelastic constant
σ	Normal stress
τ	Shear stress
S_t	Tensile Stress
S.C.	Stress concentration factor

INTRODUCTION

Photoelastic stress analysis is one of the most effective methods available to the engineer for solving problems of stress distribution. The effect of forces, such as pressure and tension may be studied using a scale model of a structural part. Special transparent models are subjected to forces proportional to those acting on the real object. The stress problem produced in the model indicates the stress distribution through a ~~cross-section~~ of the structural part.

Analysis of the photographic record of the stress analysis pattern provides data with a high degree of accuracy within a relatively short time. In simple cases, this data can be used either alone or as a check of mathematical solutions. They also yield reliable information on problems which are insolvable mathematically or at least involve complicated and tedious calculations. Examples include the stresses around notches and holes in bars, in riveted joints, spoked wheels, gear teeth and frame works with welded joints or in redundant members.

Other methods of stress analysis used in the design and testing of structural forms described briefly as follows:

BRITTLE COATING:

The structure is covered with a special coating designed to crack wherever strain exceeds a fixed

amount. This method indicates regions of dangerous stress and provides an over all picture of surface stresses. This method is mainly used to indicate the directions of the principal stresses so that electric strain gages may be accurately oriented.

ELECTRIC STRAIN GAGES:

These are the most versatile devices for use by the stress analyst. They are readily adaptable to all kinds of structures and materials. With the electronic equipment available today the variable resistance wire strain gage is without a doubt the most favorable means of measuring dynamic and transient surface strains. However, the wire is very susceptible to temperature changes whereby a thermocouple effect may be established.

Photoelastic stress analysis, however, has certain advantages:

- (1) A more complete view of the stress pattern is obtained, instead of surface stresses at a limited number of points.
- (2) Stresses in relatively inaccessible places can be studied such as points of stress concentrations.
- (3) Tests can be quickly made and inexpensively before its structural counterpart is made.

HISTORY

In 1816 Sir David Brewster published an account of his findings that clear stressed glass when examined in polarized light exhibited colored patterns. However, the application of this discovery to engineering problems was not recognized before 1900, although the underlying theory was well developed by physicists such as Neumann, Maxwell, and Wertheim who formulated the concept that the optical retardation producing the color effects is proportional to the difference of the principal stresses existing in glass.

In 1920, Professor E. G. Coker of the University of London further advanced the theory by the introduction of cellulose models and the use of monochromatic light.

However, since 1940 the introduction of other methods of stress analysis caused a decrease in the development of photoelasticity as a method of stress determination.

OPTICS

There are two basic theories that attempt to explain the behavior of light. The corpuscular theory of light is based on the assumption that light is caused by the motion of light corpuscles emitted from a light source. This theory satisfactorily explains certain phenomena, such as reflection, refraction, and the photoelectric effect. However this theory does not satisfactorily explain the phenomena of polarization, as does the earlier electromagnetic wave theory.

According to the wave theory, light is assumed to be composed of electromagnetic waves. The amplitude of the wave motion is proportional to the electric and magnetic field strengths of the wave motion. Since both electric and magnetic fields are vector quantities and in light are definitely related, the wave motion may be represented by a single vector representing either electric or magnetic field strengths. The direction of the vector ray is normal to the path of propagation of light and in the plane of the wave motion.

A beam of light is considered as being composed of a number of rays of light, each ray travelling along its path independently of the other rays but subject to the same behavior.

If a beam of light is incident upon a transparent medium capable of transmitting light that is vibrating in

in one plane only, then only the ray of light in that plane and the components of other rays in that plane will be transmitted. This is called plane polarization of light.

The following sketch shows clearly the characteristics of electromagnetic wave motion light and the effect of polarization on the light rays.

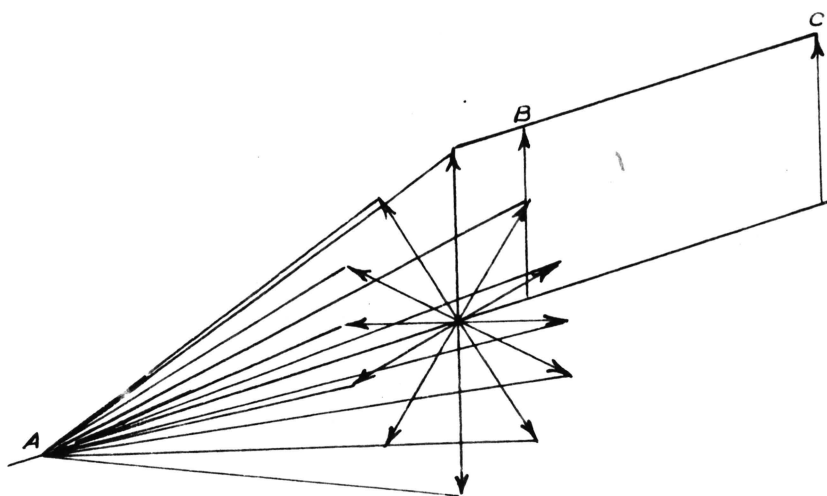


Fig. 1

S = Source of light

B = Polarizer

C = Ray of polarized light vibrating in one plane only.

The displacement of this beam of light can be expressed by the equation:

$$A = a \sin \omega t$$

Where α is the amplitude of the vibration and ω is the circular frequency.

If the ray of light is passed through a second polarizer whose plane of polarization is at an angle θ with the first polarizer, the component of the ray of light that is passed by the second polarizer, known in photo-elastic work as the analyzer, may be expressed by the equation:

$$A_1 = \alpha \cos\theta \sin \omega t$$

This indicates that as the analyzer is rotated from 0° to 90° that the light passing the analyzer will vary from a maximum at 0° to zero at 90° .

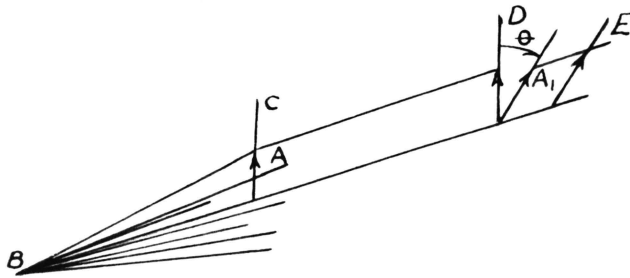


Fig. 2

- B = Light source
- C = First polarizing agent (polarizer)
- D = Second polarizing agent (analyzer)
- E = Observing screen

A = Amplitude of light passed by C

A_1 = Amplitude of light passed by D

If the light passing the first polarizer is incident on a double refracting material, oriented at an angle θ with the polarizer, the equation of the displacement of the light passed now becomes:

$$A_1 = a \cos\theta \sin\omega t$$

and $A_2 = a \sin\theta \sin\omega t$

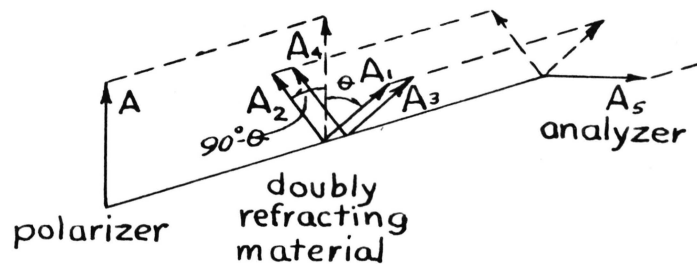


Diagram showing double-refracting material between polarizer and analyzer.

Fig. 3

A double refracting medium is one in which a beam of light is divided into two beams, one beam passing through the medium more rapidly than the other. This phenomena is due to the different indices of refraction of the medium. Because of the different indices of refraction of a material, the components of light emerging will have developed a phase difference so that:

$$A_3 = \alpha \cos\theta \sin \omega (t + \delta t) \quad (6)$$

and $A_4 = \alpha \sin\theta \sin \omega t \quad (7)$

The light passed by the analyzer then becomes:

$$A_5 = \alpha \sin 2\theta \sin \frac{\omega \delta t}{2} \cos \left(\omega t + \frac{\omega \delta t}{2} \right) \quad (8)$$

The time difference δt is a result of the difference in transmission velocities through a double refracting material. If v is the velocity of light in air and N_1 and N_2 are the indices of refraction then:

$$t_1 = N_1 d / v \quad (9)$$

and $t_2 = N_2 d / v \quad (10)$

where d is the model thickness

so that $\delta t = \frac{d}{v} (N_1 - N_2)$

$$\omega \delta t = \frac{\omega d}{v} (N_1 - N_2) = \frac{2\pi d}{\lambda} (N_1 - N_2) \quad (11)$$

where $\lambda = \frac{2\pi v}{\omega} \quad (12)$

If f is considered to be the number of wave lengths of relative retardations then:

$$\omega \delta t = 2\pi f = \frac{2\pi d}{\lambda} (N_1 - N_2) \quad (13)$$

$$f = \frac{d}{\lambda} (N_1 - N_2) \quad (14)$$

By experiment it has been found that the change in the refractive index of a material is proportional to the intensities of the principal stresses. The light polarized in the directions of the principal stresses is transmitted only on the planes of principal stress.

$$f = \frac{d}{C} (\sigma_1 - \sigma_2) \quad (15)$$

Where C is the photoelastic constant of the material which is a characteristic constant for each material so .

$$A_5 = \alpha \sin 2\theta \sin \frac{\pi d}{C} (\sigma_1 - \sigma_2) \cos \left(\omega t + \frac{2\pi d}{C} (\sigma_1 - \sigma_2) \right) \quad (16)$$

As can be seen by equation (16) if the angle θ is equal to either zero or 90° , whereby the plane of polarization of the light is parallel to a principal stress axis direction, no light will pass through the analyzer. This will produce black lines known as isoclinics. If the principal stress difference is such that:

$$\sin \frac{\pi d}{C} (\sigma_1 - \sigma_2) \quad (17)$$

will equal either zero or π or if the

$$\frac{\pi d}{C} (\sigma_1 - \sigma_2) \quad (18)$$

term is equal to any multiple integer of π no light will reach the screen. This condition will also produce black lines known as isochromatics if a monochromatic light source is used.

To remove the isoclinic lines from the screen, quarter wave plates must be introduced. These are transparent sheets of mica oriented at a 45° angle to the polarizer and of such thickness that they produce a retardation of one quarter of a wave length, causing circularly polarized light.

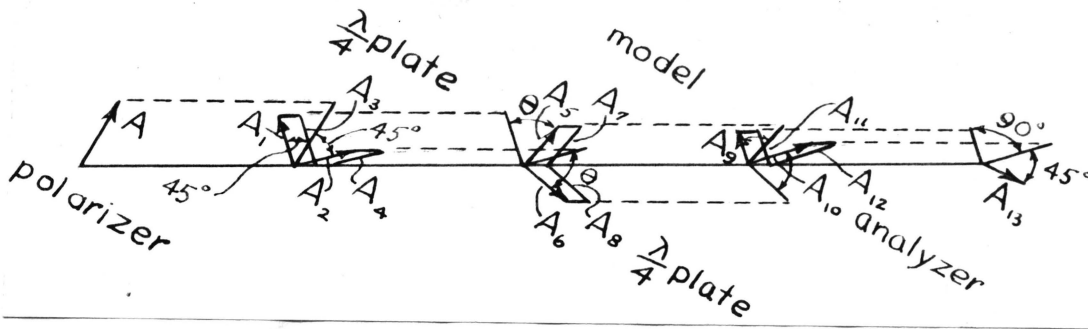


Fig. 4

From Fig. 4 it can be seen that the light that passes through the quarter wave plate and falls on the model will be:

$$A_3 = .706 \alpha \sin (\omega t + 90^\circ) \quad (19)$$

$$A_4 = .707 \alpha \sin \omega t \quad (20)$$

These components of the circularly polarized light passing through the model are resolved into new components parallel to the principal stress directions so that:

$$A_5 = .707 \alpha \sin (\omega t + 90^\circ + \theta) \quad (21)$$

$$A_6 = .707 \alpha \sin (\omega t + \theta) \quad (22)$$

Then those components entering the quarter wave plates are now:

$$A_7 = .707 \alpha \sin (\omega t + 90^\circ + \theta + \omega \delta t) \quad (23)$$

$$= -.707 \alpha \cos (\omega t + \theta + \omega \delta t) \quad (24)$$

$$A_8 = .707 \alpha \sin (\omega t + \theta) \quad (25)$$

After passing through the next quarter wave plate

$$A_{11} = -.707 \alpha \cos \theta \cos (\omega t + \theta + \omega \delta t + 90^\circ) \quad (25)$$

$$= -.707 \alpha \sin \theta \sin (\omega t + \theta + 90^\circ) \quad (26)$$

$$\begin{aligned}
 A_{12} &= -.707 \alpha \sin \theta \cos (\omega t + \theta \omega \delta t) \\
 &\quad + .707 \alpha \cos \theta \sin (\omega t + \theta)
 \end{aligned}
 \tag{27}$$

Then the light transmitted by the analyzer will be

$$A_{13} = \alpha \cos \frac{\omega \delta t}{2} \sin \left(\omega t + \frac{\omega \delta t}{2} \right)
 \tag{28}$$

Since the angle θ does not appear in the equation, the light passed by the analyzer is independent of the orientation of the principal stress directions of the model, which eliminates the isoclinics.

By various substitutions as previously made

$$A_{13} = \alpha \cos \frac{\pi d}{c} (\sigma_1 - \sigma_2) \sin \omega t + \frac{\pi d}{c} (\sigma_1 - \sigma_2)
 \tag{29}$$

STRESS

Since the photoelastic effects are related to the principal stresses it is advisable to show the relationship between stresses on the various planes that may be passed through any given point in a body. The relationships among the stresses on various planes passing through a point may be determined by applying the equations of equilibrium to a free body diagram of an element.

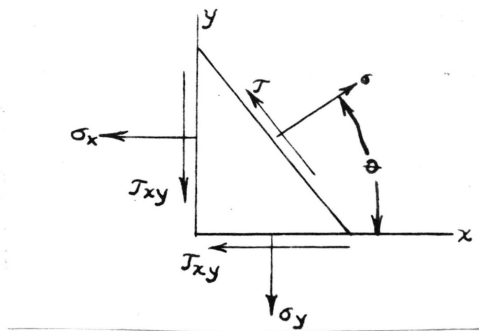


Fig. 5b

Stresses at a point in a two dimension system.

By the summation of forces it can be seen that

$$\begin{aligned} \sigma &= \sigma_x \delta y \delta z \sin\theta + \tau_{xy} \delta y \delta z \cos\theta + \sigma_y \delta x \delta z \cos\theta \\ &\quad + \tau_{xy} \delta x \delta z \sin\theta \end{aligned} \quad (1)$$

and since $\delta y \delta z$ is the $\sin\theta$ and $\delta x \delta z$ is the $\cos\theta$

$$= \sigma_x \sin^2\theta + 2\tau_{xy} \sin\theta \cos\theta + \sigma_y \cos^2\theta \quad (2)$$

$$= 1/2 (\sigma_x - \sigma_y) + 1/2 (\sigma_x - \sigma_y) \cos 2\theta + \tau_{xy} \sin 2\theta \quad (3)$$

In a similar manner it can be found that

$$\tau = 1/2 (\sigma_x - \sigma_y) \sin 2\theta + \tau_{xy} \cos 2\theta \quad (4)$$

By differentiating equation 3 and setting the result equal

to zero it will be found that

$$\tan 2\theta = \frac{2\tau_{xy}}{\sigma_x - \sigma_y} \quad (5)$$

from this it can be seen that when σ is maximum and τ becomes zero, so that the algebraic maximum and minimum normal stresses lie on planes where there is no shearing stress, the normal stresses are then principal stresses. Since there are two possible values for the angle 2θ which are 180° apart there are two principal stresses lying on planes 90° from each other.

If the values of the principal stresses are found by substituting values from equation 5 into equation 3 and 4, the following relations are obtained:

$$\begin{aligned} \sigma_1 &= 1/2 (\sigma_x + \sigma_y) + 1/2 [(\sigma_x - \sigma_y)^2 + 4\tau_{xy}^2]^{1/2} \\ \sigma_2 &= 1/2 (\sigma_x + \sigma_y) - 1/2 [(\sigma_x - \sigma_y)^2 + 4\tau_{xy}^2]^{1/2} \\ \tau_m &= 1/2 [(\sigma_x - \sigma_y)^2 + 4\tau_{xy}^2]^{1/2} \\ &= 1/2 (\sigma_1 - \sigma_2) \end{aligned} \quad \begin{matrix} (6) \\ (7) \\ (8) \\ (9) \end{matrix}$$

So that the maximum shearing stress at any point is equal to $1/2$ the difference of the principal stresses.

By comparing equation (9) with equation (11) from the previous section on Optics it can be seen that isochromatics are regions of constant maximum shear stress.

**PROBLEM
AND
PROCEDURE**

The author's problem was the investigation of stress concentrations at notched corners of square apertures in flat plates subjected to tension. Previous work along this line had been done by R. H. Beaver. (1) He investigated the stress concentration at filleted corners

(1) Beaver, R. H. Thesis Missouri School of Mines
1951

of square apertures in flat plates subjected to tension.

The problem was divided into two parts. For the first part a flat plate of constant length, width, thickness, and aperture size was used varying only the diameter of the notch. In the second part the notch remained constant at 0.125 inches and the plate varied in width and aperture size maintaining at the same time a constant ratio between the plate width and aperture size of 2.67. This ratio of plate width and aperture size was held constant as any variation would affect the stress concentration.

The models were constructed from clear catalin, a phenolformaldehyde condensate similar to bakelite, 6 inches long, 1 inch wide, and $7/32$ inch thick. Models of this small size were used in order to obtain a maximum

amount of fringe lines without fracturing the material at the supports. It is interesting to note that the models failed at the $3/8$ inch hole drilled so that the model could be supported in tension. This is because of the fact that the stress caused by the hole is 3 times the stress without the hole. (2).

(2) Timoshenko, Theory of Elasticity p. 78, 1934

The equipment used was standard photoelastic apparatus consisting of polaroids, quarter wave plates, monochromatic light source and an attached camera. Photographs were made with 5 x 7 inch Super Ortho-Press Film at $1/25$ th of a second exposure. The photographs were enlarged to facilitate counting fringes.

In order to determine the maximum fringe order at the boundary, the fringes were plotted against the percent distance to the edge and the curve extrapolated.

The photoelastic constant of the material was determined by finding the change in fringe order caused by a variation of the load.

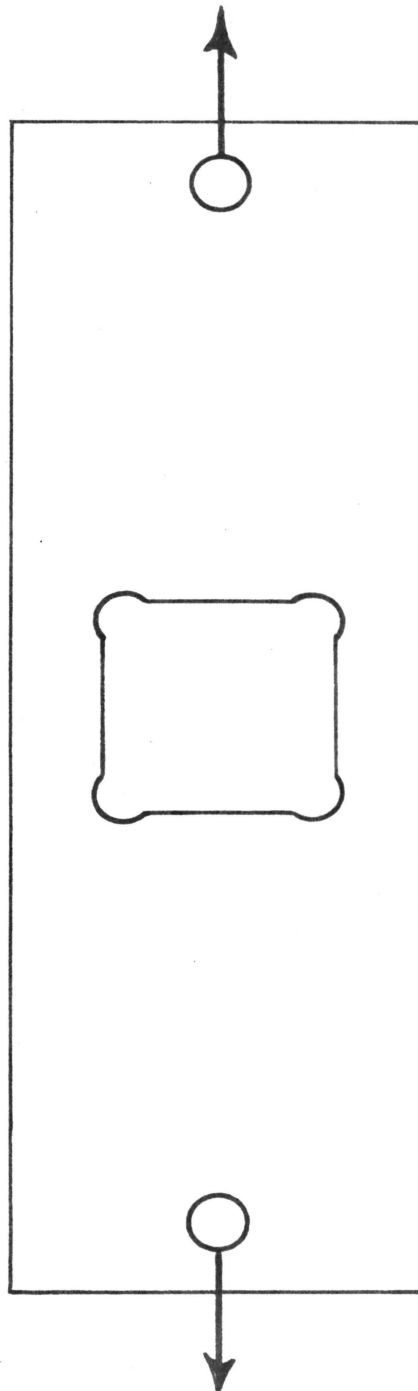


Figure 7

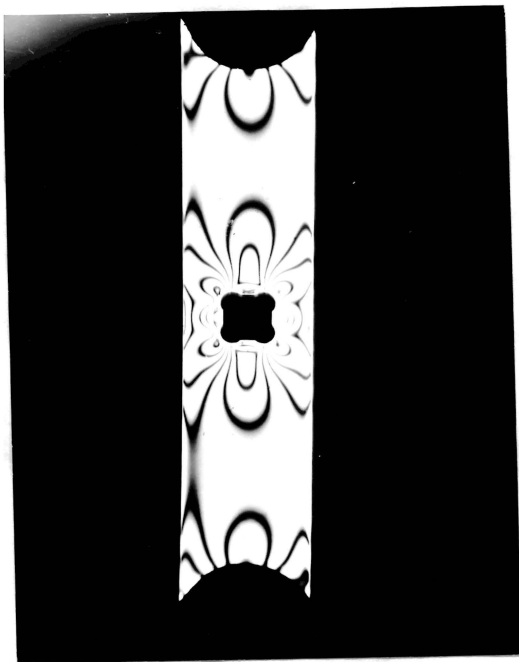


Figure 8

MODEL #1

Width = 1 inch
 Length = 6 inches
 Thickness = 0.2065 inches
 Notch Diam. = 0.187 inches
 Hole Size = 0.375 in. sq.
 Load = 259 pounds
 Fringe Order = 11.4

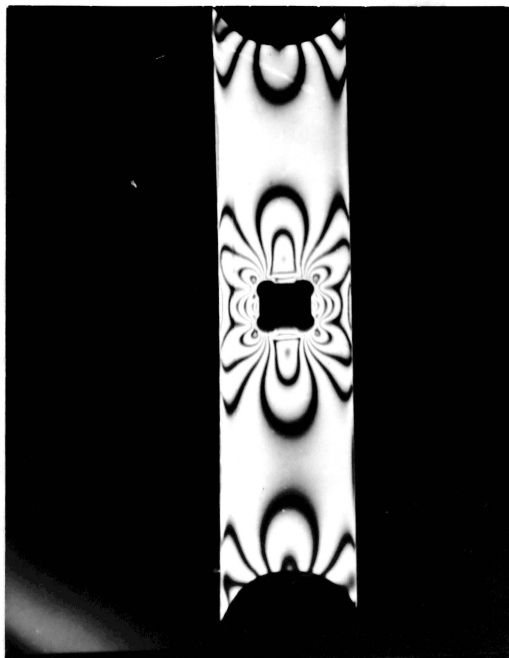


Figure 9

MODEL #2

Width = 1 inch
 Length = 6 inches
 Thickness = 0.2175 inches
 Notch Diam. = 0.156 inches
 Hole Size = 0.375 in. sq.
 Load = 299 pounds
 Fringe Order = 10.8

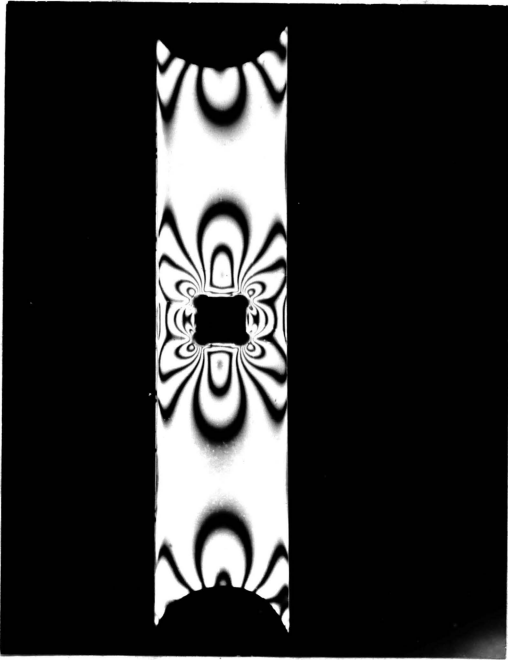


Figure 10

MODEL #3

Width = 1 inch
 Length = 6 inches
 Thickness = 0.2165 inches
 Notch Diam. = 0.125 inches
 Hole Size = 0.375 in. sq.
 Load = 299 pounds
 Fringe Order = 8.5

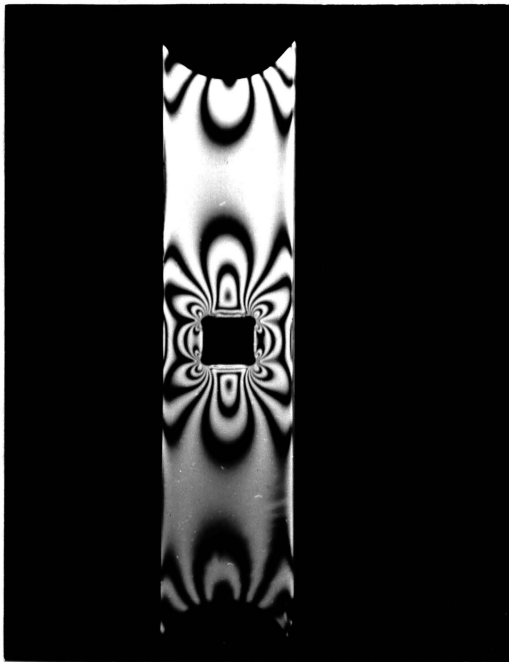


Figure 11

MODEL #4

Width = 1 inch
 Length = 6 inches
 Thickness = 0.2145 inches
 Notch Diam. = 0.093 inches
 Hole Size = 0.375 in. sq.
 Load = 299 pounds
 Fringe Order = 9.2

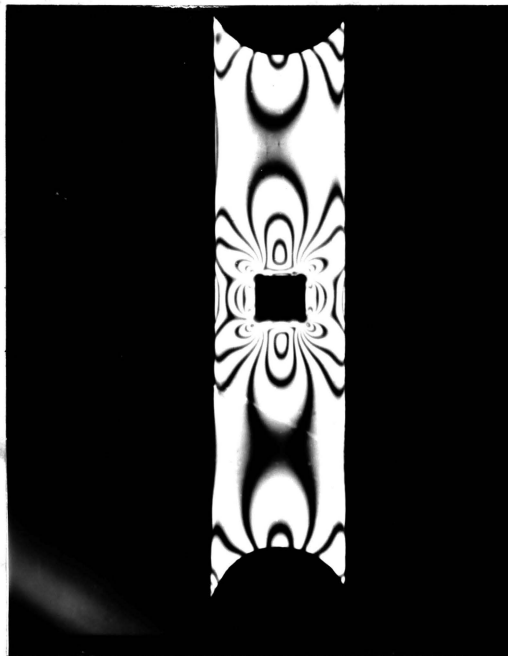


Figure 12

MODEL #5

Width = 1 inch
Length = 6 inches
Thickness = 0.2065 inches
Notch Diam. = 0.076 inches
Hole Size = 0.375 in. sq.
Load = 299 pounds
Fringe Order = 9.2

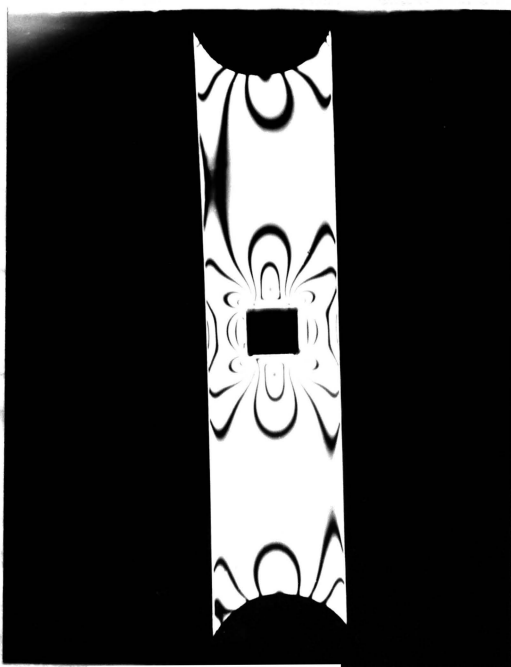


Figure 13

MODEL #6

Width = 1 inch
Length = 6 inches
Thickness = 0.208 inches
Notch Diam. = 0.040 inches
Hole Size = 0.375 inches
Load = 299 pounds
Fringe Order = 10.2

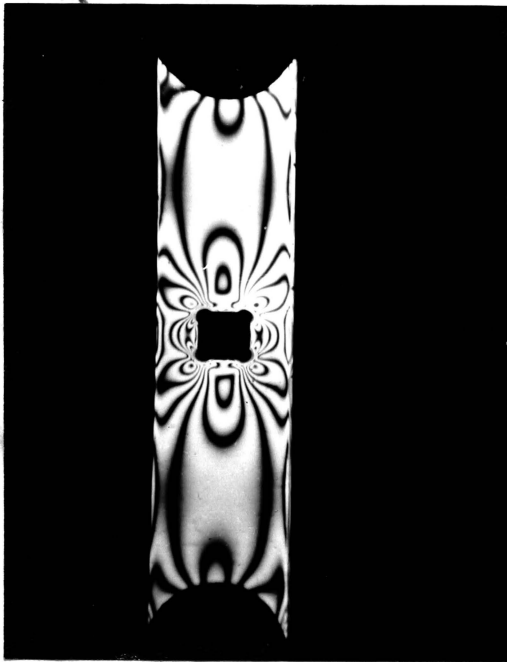


Figure 14

MODEL #7

Width = 1.068 inches
Thickness = 0.2075 inches
Notch Diam. = 0.125 inches
Hole Size = 0.4 in. sq.
Load = 299 pounds
Fringe Order = 8.4

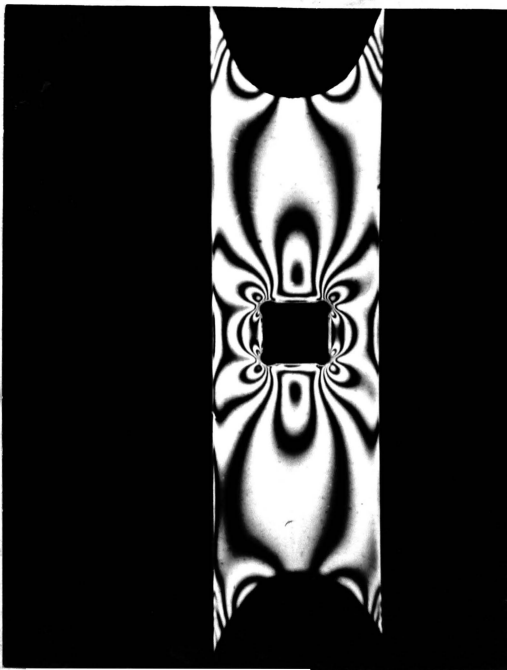


Figure 15

MODEL #8

Width = 1.333 inches
Thickness = 0.2045 inches
Notch Diam. = 0.125 inches
Hole Size = 0.5 in. sq.
Load = 299 pounds
Fringe Order = 7.4

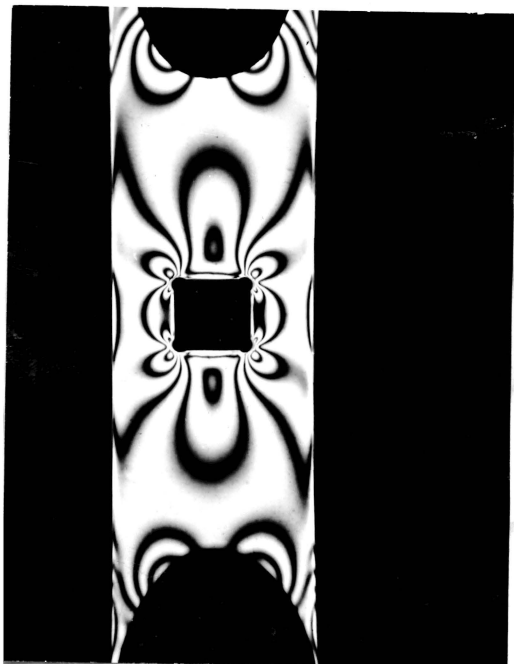


Figure 16

MODEL #9

Width = 1.600 inches
 Thickness = 0.203 inches
 Notch Diam. = 0.125 inches
 Hole Size = 0.6 inches
 Load = 299 pounds
 Fringe Order = 5.6

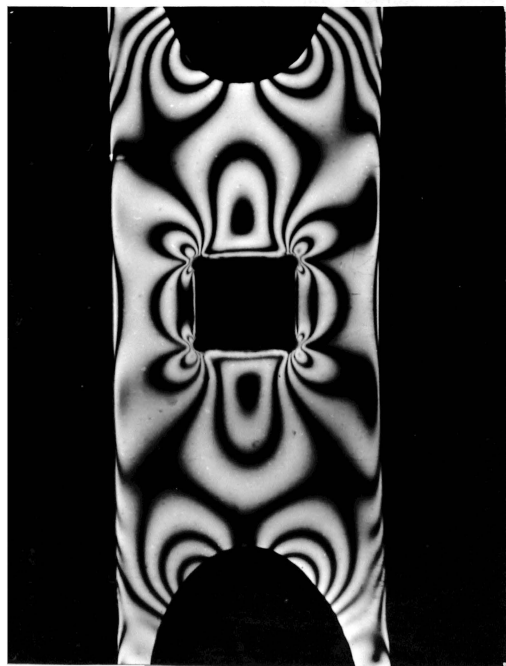


Figure 17

MODEL #10

Width = 2.00 inches
 Thickness = 0.2193 inches
 Notch Diam. = 0.125 inches
 Hole Size = 0.75 inches
 Load = 419 pounds
 Fringe Order = 7.5

CALCULATIONS

The tensile stress in a model having a hole in it is equal to:

$$St' = \frac{(\text{Optical Constant}) \times (\text{Fringe Order}) \times 2}{(\text{Thickness of plate})}$$

Example: Model #6

$$St' = \frac{50 \times 10.2 \times 2}{.208} = 4910 \text{ psi.}$$

The tensile stress expected in a model

$$St = \frac{\text{Load}}{\text{Area}} = \frac{299}{0.625 \times 0.208} = 2310 \text{ psi.}$$

The stress concentration factor is equal to:

$$S.C. = St' / St = 4910 / 2310 = 2.12$$

DATA FOR FIRST TEST

Width of plate = 1 inch

Length of plate = 6 inches

Hole Size = 0.375 inches square

Optical constant = 50 psi / inch

TABLE 1

MODEL #	NOTCH DIAM.	LOAD	FRINGE ORDER	STRESS S_t'	STRESS S_t	S.C.
1	0.187	259	11.4	5520	2005	2.75
2	0.156	299	10.8	4960	2200	2.26
3	0.125	299	8.5	4080	2210	1.84
4	0.093	299	9.2	4290	2230	1.92
5	0.076	299	9.2	4320	2320	1.92
6	0.040	299	10.2	4910	2310	2.12

Notch diameter in inches

Load in pounds

Stress S_t' is the tensile stress determined from fringes

Stress S_t is the stress on a plate neglecting corner concentration.

S.C. is the stress concentration factor.

DATA FOR SECOND TEST

Length of plate = 6 inches

Width of plate / width of hole = 2.67

Notch diameter = 0.125 inches

Optical constant = 50 psi / inch

TABLE 2

MODEL #	HOLE SIZE	LOAD	FRINGE ORDER	STRESS S_t'	STRESS S_t	S.C.
3	0.375	299	8.5	4080	2210	1.84
7	0.400	299	8.4	4050	2610	1.88
8	0.500	299	7.4	3660	1755	2.06
9	0.600	299	5.6	2760	1470	1.88
10	0.750	419	7.5	3430	1525	2.25

Hole size in inches

Load in pounds

Stress S_t' is the tensile stress determined from fringes

Stress S_t is the stress on a plate neglecting corner
concentration.

S.C. is the stress concentration factor.

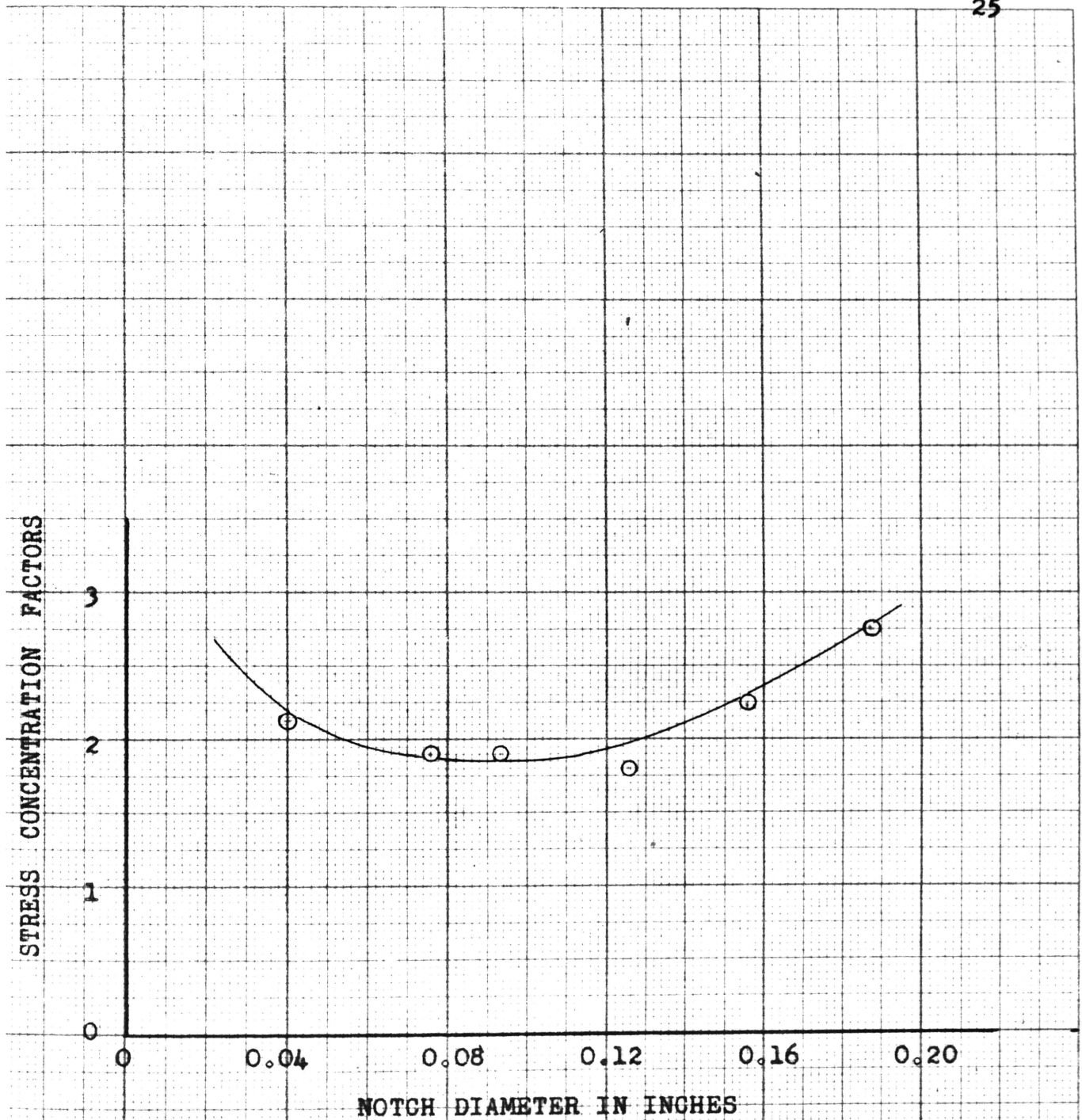
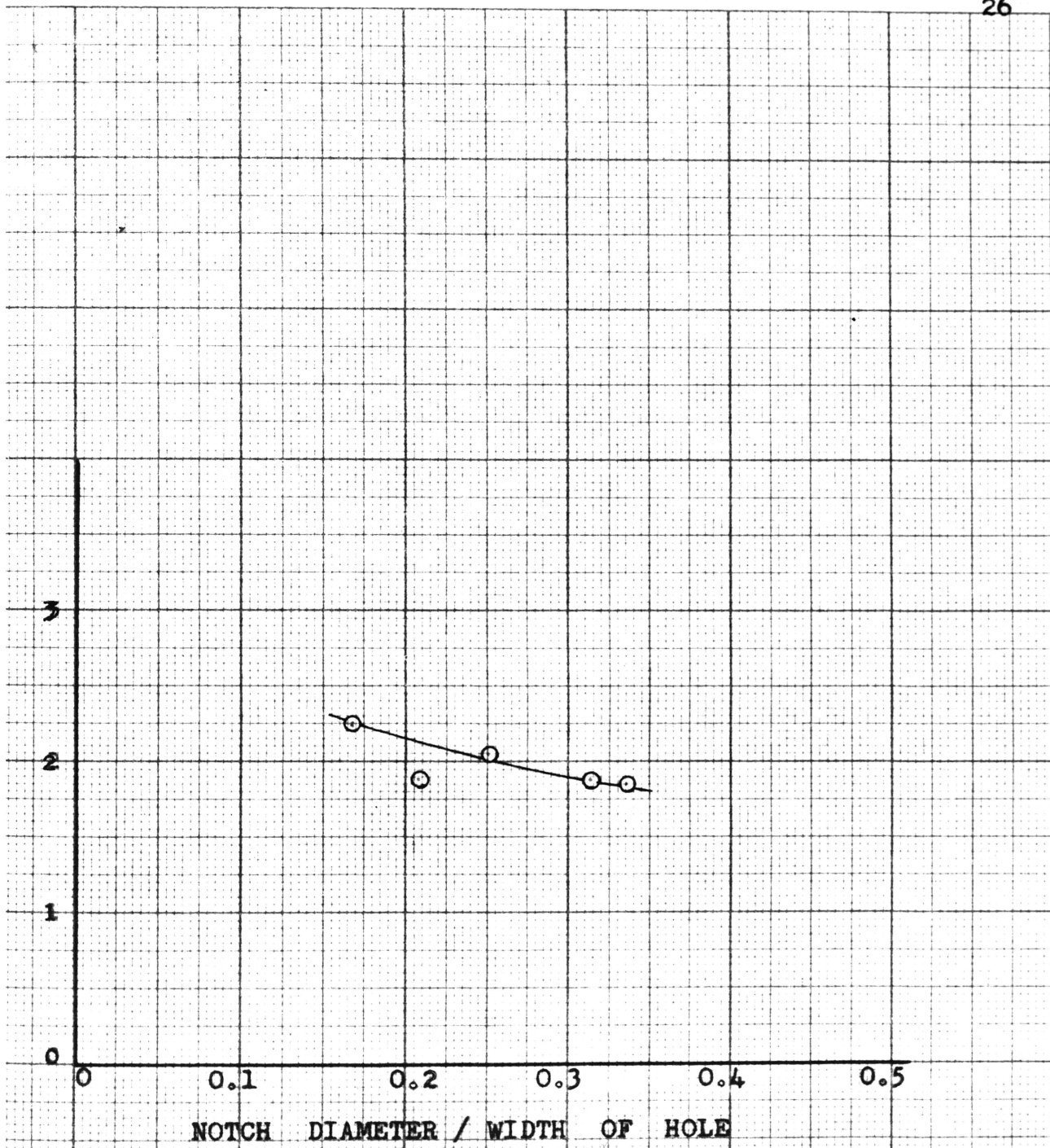


PLATE 1: STRESS CONCENTRATION FACTORS AT NOTCH

WIDTH OF PLATE = 1 INCH

LENGTH OF PLATE = 6 INCHES

SIZE OF HOLE = 0.375 INCHES SQUARE



LATE 2: STRESS CONCENTRATION FACTORS AT NOTCH

NOTCH DIAMETER = 0.125 INCHES

LENGTH OF PLATE = 6 INCHES

CONCLUSIONS

The results of the problem are rather interesting in that the notches of diameters $3/16$ inch to $1/8$ inch cause the point of maximum stress to move from the expected point at the hole corner to the vertical sides of the hole. This is caused by the larger notches creating another re-entrant corner where they enter the hole and has the effect of a knee frame. For notches of smaller diameters than $1/8$ inch the points of maximum stress appear at the edges of the hole corners.

Plate #2 shows the effect of holding the notch diameter constant and varying the size of the hole. It can be seen that as the size of the hole is increased the stress concentration increases slightly.

BIBLIOGRAPHY

1. Books:

Frocht, M. M. Photoelasticity. Vol. 1. N. Y. Wiley
1949. 411 p.

Hetenyi, M. Handbook of Experimental Stress Analysis
N. Y. Wiley 1950. pp. 828-924.

Lee, G. A. An Introduction to Experimental Stress
Analysis. N. Y. Wiley 1950. pp. 148-224.

Timoshenko, S. Theory of Elasticity. N. Y. McGraw Hill
1934. pp. 1-135.

2. Unpublished Material:

Bever, R. H. Photoelastic Investigation of Filleted
Corners in Square Apertures in Flat Plates Subjected
to Tension. Thesis, Missouri School of Mines and Metal-
lurgy, Rolla, Mo., 1951.

VITA

Lloyd E. Byrd, Jr. was born in Worcester, Massachusetts on the 5th day of September, 1925. He received his elementary education at Worcester, Massachusetts.

After spending two years in the army, he attended La Salle-Peru Junior College, La Salle, Illinois. In 1948 he transferred to the Missouri School of Mines and Metallurgy, Rolla, Missouri, where he received his Bachelor of Science degree in Mechanical Engineering in the year 1950.

